

Investigation of microstructure and mechanical properties of low carbon steel sheets after severe plastic deformation in corrugation dies

F. Khodabakhshi^{1*}, M. Kazeminezhad², A. H. Kokabi³

Department of Materials Science and Engineering Sharif University of Technology, Azadi Ave., Tehran, Iran

Abstract

Recently, bulk nano-structured materials produced by severe plastic deformation (SPD) have attracted scientists attention. Materials produced by SPD are of great importance because of (1) non-porous structure, (2) great mechanical properties such as high strength and toughness and (3) proper dimension for mechanical and physical testing. Several methods have been introduced for imposing the severe plastic deformation on the metals. In this research, pressing in corrugation dies is carried out on the sheets of low carbon steel at room temperature. The potential of this method in grain refinement and mechanical properties improvement of low carbon steel sheets is investigated using XRD, tensile and hardness tests. The results show that in strain magnitude of 4.64, a microstructure with a grain size of 230 nm is achieved.

Keywords: Severe plastic deformation, Low carbon steel, Corrugation die, Mechanical properties, Microstructure.

1. Introduction

In recent years, bulk nano-structured materials processed by methods of severe plastic deformation (SPD) have attracted materials scientists,¹⁾ attention and several methods have been introduced for this purpose²⁾. Ultra fine grained (UFG) materials can be synthesized by either bottom-up or top-down approaches. In the bottom-up approach, the nanostructure is produced through atom-by-atom and layer-by-layer arrangement. This approach often leads to a porous structure and is not applicable to industrial manufacturing³⁾. In the top-down approach, the bulk microstructure of material is changed to nanostructure by means of severe plastic deformation (SPD)⁴⁾. Samples produced by this method have a desirable property for automobile industry because of their high strength to weight ratio. Since the SPD processes refine the grain size of materials into nano-scale, the transmission electron microscopy (TEM) and X-ray diffraction (XRD) two basic methods for grain size evaluation of processed materials⁵⁾. Transmission electron microscopy can provide a direct image of the grain size distribution. However, the reliability of images depends on whether the thin area is a representative of the original microstructure of the entire sample.

XRD advantages include: Large sampling volume, non-destructiveness and simple interpretation of its result. Also, using XRD makes it possible to monitor the

microstructural changes during SPD processes^{5,6)}.

The principle of SPD includes an increase dislocation density by heavily uniform deformation of materials, formation of dense dislocation walls, and transformation of dislocation walls into high-angle grain boundaries⁷⁾. Materials produced by SPD are of great importance due to their non-porous structure, great mechanical properties and proper dimension for mechanical and physical testing⁸⁾. Two major SPD processes of sheet are accumulative roll banding (ARB) and pressing in corrugation dies. ARB process has some disadvantages such as imperfect bonding between layers of sheet or edge cracking during rolling process which limit its applications⁹⁾. In 2002 Shin et al. invented an other SPD process of sheet pressing in corrugation dies which consists of repetitive shear deformation under plane strain deformation condition by utilizing alternate pressings with corrugation and flat dies (Fig. 1)¹⁰⁾. Since the SPD of low carbon steel is important and ARB has some disadvantages, in this research, pressing in corrugation dies method is carried out on the sheets of low carbon steel. In this study, strain magnitudes of 0 to 4.64 are imposed on the low carbon steel sheets to produce a high strength nano-structured sheet and in the following experiment, tensile and hardness tests, characteristics of deformed sheets are investigated by using XRD.

2. Experimental Procedure

A low carbon steel sheet with dimensions of 84mm×50mm×3mm was used to study the effectiveness of pressing in corrugation dies process for grain refining and strengthening of low carbon steel sheets. The chemical composition of the material is shown in Table 1. Schematic diagrams of corrugation and flat dies are shown in Fig. 1. Teflon layers were used as lubricants between

*Corresponding author:

Tel: +98-91-73234988 Fax: +98-21-66005717

E-mail: farzad_khodabakhshi83@yahoo.com

Address: Dept. of Materials Science and Engineering
Sharif University of Technology, Azadi Ave., Tehran, Iran
1. M.Sc

2. Assistant Professor

3. Professor

low carbon steel sheet and dies ⁷⁾. Each time the work pieces are pressed between the corrugation dies, under plane strain condition, an effective strain of 0.58 is imposed on the inclined regions while the flat regions undergo no deformation (Fig. 1(b)). Then, the work piece is removed from the dies and is flattened by means of a set of flat dies resulting in another 0.58 effective strain in reverse direction which ends up in 1.16 strains for the deformed regions (Fig. 1(c)). After the flattening, the specimen is rotated 180° around the axis perpendicular to the plane of the sheet (Fig. 1(d)) which ensures that the subsequent pressing (Fig. 1(e)) and flattening (Fig. 1(f)) impose an overall strain of 1.16 on the undeformed regions. After this step, a uniform strain of 1.16 is imposed throughout the specimen. In the present study, one pass is equivalent to two-corrugation pressing and two flattening stages which lead to a uniform strain on the sheet. Fig. 2 shows the processed sample sheet after the first pressing stage.

Tensile and hardness tests were carried out to investigate the mechanical behavior of low carbon steel sheets after pressing in corrugation dies. Tensile testing specimens were machined according the ASTM E8M standard and the gage length was aligned along the longitudinal direction of the pressed sheet.

XRD measurements were carried out on a Philips X-ray diffractometer to investigate the microstructure evolution of sheets during process and the results were analyzed using Williamson–Hall method. The X-ray patterns of

processed samples were measured at a step width of 0.02° and full-width at half-maximum (FWHM) for all peaks was measured using the software configured with the XRD system. For calibration of the instrumental line broadening, a full mixture of coarse TiC and B₄C powders was tested in the same condition.

Grain size and lattice micro strain can be accordingly determined by measuring the deviation of line profile from perfect crystal diffraction. For example, the Williamson–Hall equation can calculate strain and crystalline size of materials as follows ¹¹⁾:

$$B \cos \theta = \frac{K\lambda}{t} + f(\varepsilon) \sin \theta \quad (1)$$

Where B is the integral breadth of the XRD profile, K is the Scherer constant, t is the crystallite size, λ is the wavelength of X-ray, ε is the lattice strain, θ is the Bragg angle and f is a strain function. In principle, the experimental profile is the convolution of the instrumental profile and the intrinsic profile. The intrinsic profile can be obtained by unfolding the experimental profile. To do so, the Gaussian assumption is considered ⁵⁾:

$$B_{\text{exp}}^2 \cong B^2 + B_{\text{ins}}^2 \quad (2)$$

where B_{exp} , B , and B_{ins} are the integral breadth of experimental profile, intrinsic profile, and instrumental profile, respectively. Typical XRD pattern of low carbon steel is shown in Fig. 3.

Table 1. Chemical composition of low carbon steel sheet (wt%).

Fe	Base	C	0.0527	Si	0.0229
Mn	0.203	P	0.006	S	0.0031
Cr	0.0088	Ni	0.0281	Mo	0.0024

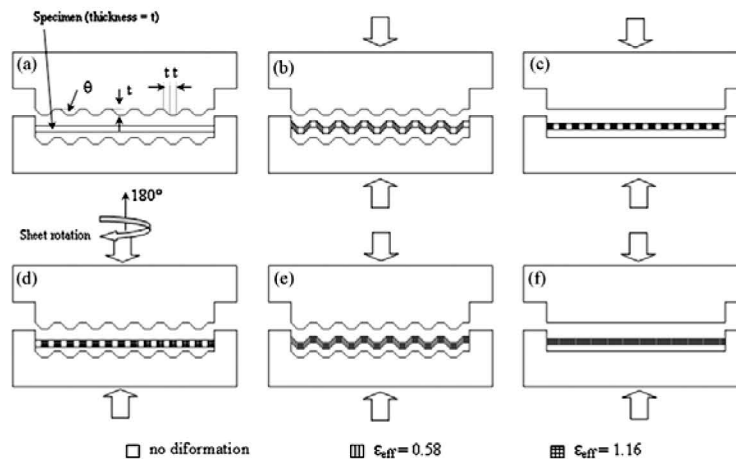


Fig. 1. Schematics of pressing in corrugation and flattening dies²⁾.

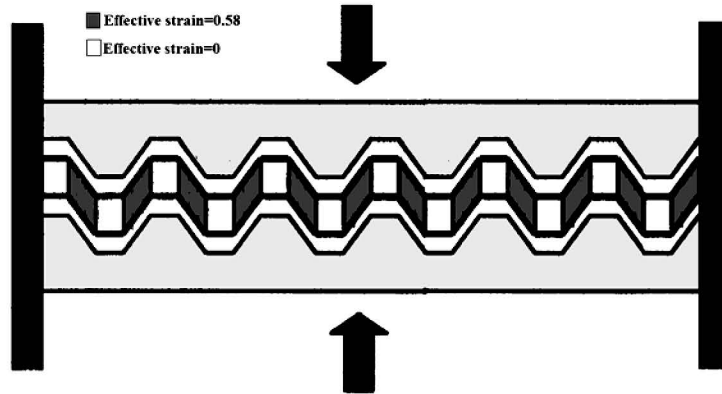


Fig. 2. Low carbon steel sheet after the first stage of pressing in corrugation die ($\epsilon_{eff}=0.58$).

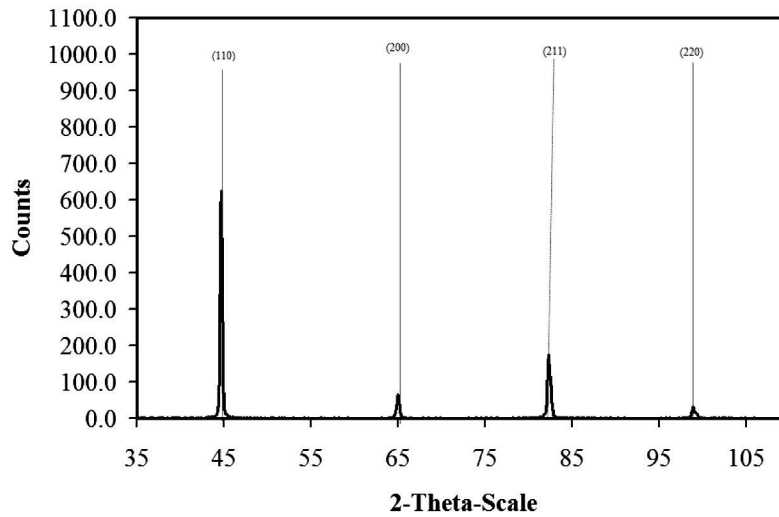


Fig. 3. X-ray diffractogram of low carbon steel after fourth passes.

3. Results and Discussion

3.1. Microstructure investigations

Analyzing the XRD patterns, evolution of low carbon steel grain size during pressing in corrugation dies process is calculated and shown in Fig. 4. As can be seen, during first pass of this method, the coarse grained low carbon steel (with average grain size of $30\mu\text{m}$) refines to a structure with a cell size of 346 nm . However, after this rapid refinement, the rate of refining is decreased and after the fourth pass, the cell size is approximately 230 nm .

Dislocation theories can interpret this trend; a relationship between imposed strain rate and rate of dislocation generation is obtained if the Orowan equation is considered on a larger time scale ⁷⁾:

$$\dot{\rho}^* = \frac{\dot{\gamma}}{bL} \quad (3)$$

$$d \propto \frac{l}{\sqrt{\rho}} \quad (4)$$

Where $\dot{\rho}^*$ is the rate of dislocation density increasing; L is the dislocation free path; b is the Burgers vector and $\dot{\gamma}$ is the resolved strain rate. By considering Eq. (3) and (4), it seems that deformation can refine the structure in a uniform manner. However, the second type of dislocation reactions during deformation, called dynamic recovery, prohibits this steady rate grain refinement. The main role of dynamic recovery is dislocation annihilation and since the rate of dynamic recovery is proportional to the material dislocation density, it is increased through straining

and it causes the rate of grain refinement to decrease at large strains. Therefore, it is acceptable to observe intensive grain refinement at the initial passes of pressing in corrugation dies and the reduced rate of refinement at the following passes.

Comparing the TEM observations reported by Fukuda et al.¹²⁾ in the ECAE of the same composition steel with the achieved results of XRD analysis shows that both processes have similar effects on grain size evolution of carbon steel.

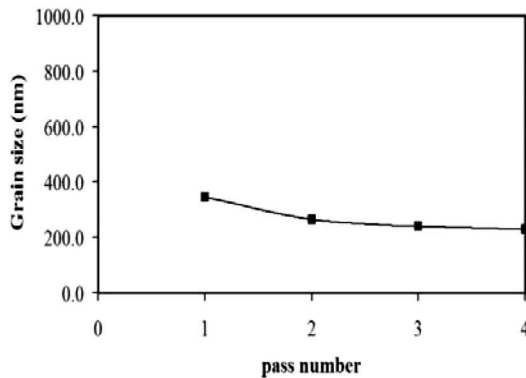


Fig. 4. The grain size versus pass number.

3.2. Mechanical properties

Hardness distribution along the specimen length for each pass after severe plastic deformation at room temperature is shown in Fig. 5. In Fig. 6, mean hardness values are plotted as a function of pass number. Hardness measurements are made on the plane perpendicular to the pressing direction. The initial material has an average hardness of 97.8 VHN, while pressing in corrugation dies increases the hardness to 180.6 VHN. The hardness values are continuously increased with increasing number of passes. Hardness variations across the length of the sample are more after the first pass and hardness inhomogeneity is decreased with an increase in the pass number.

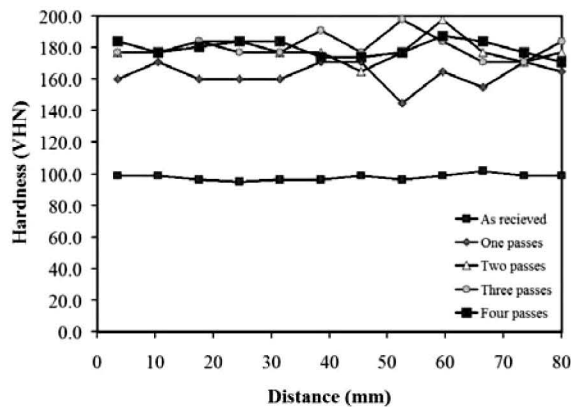


Fig. 5. The Vickers hardness profile along the length of sheet.

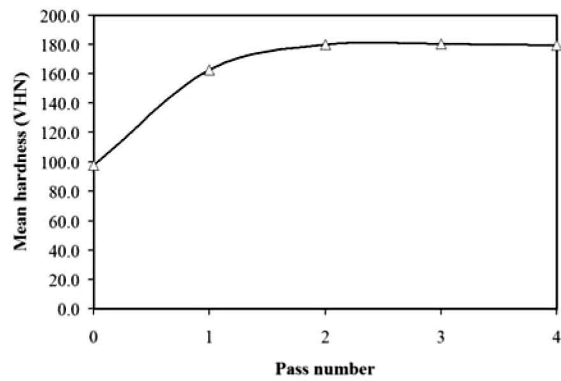


Fig. 6. The hardness of sheets versus pass number.

The tensile properties of deformed sheets are shown in Fig. 7. The as-received sheet has an ultimate tensile strength of 288 MPa. After two passes of pressing in corrugation dies, ultimate tensile strength is increased from 288 MPa to 447 MPa. The yield strength of the as-received sheet is 204 MPa and after the first pass, the yield strength is increased to 412 MPa. Increasing the strength of material during SPD is common and arises from work hardening and grain refining mechanisms. However, dropping of strength at the second pass requires more investigations. Previous papers explained this phenomenon using two theories; micro-cracking and flow softening^{7, 10)}. The percentage of elongation at fracture is decreased from 39% for as-received sheet to 10.3% after the fourth passes.

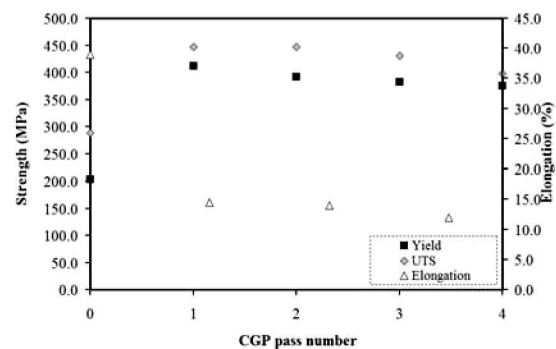


Fig. 7. Tensile properties of produced steel sheets.

Figs. 8 and 9 show the tensile behavior of annealed and two-pass deformed samples, respectively. From these figures, it can be observed that deformation through this process leads to a decrease in uniform elongation of samples from 0.259 to 0.022. It means that plastic instability starts earlier in the pressed material in corrugation dies and necking occurs in preliminary stages of tensile deformation. The early onset of necking in the pressed material is due to the low-hardening rate¹³⁾. However, it can be seen that

the magnitude of non-uniform elongation is markedly increased after pressing in corrugation dies process. This means that major tensile strains are obtained in the state of plastic instability, and that the material has high strain rate sensitivity¹³. These evidences indicate that plastic deformation through pressing in corrugation dies increases the super-plasticity tendency of low carbon steel sheets that is acceptable considering the grain refinement during this process.

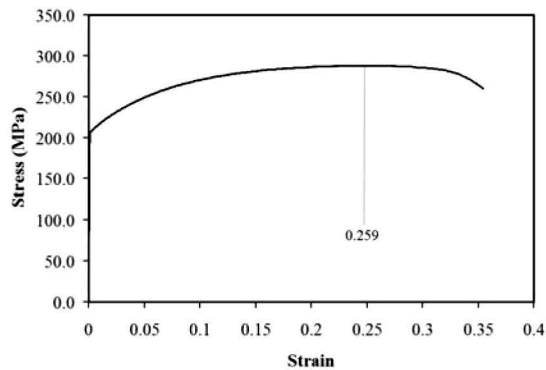


Fig. 8. Stress-strain curve of as-received low carbon steel sheet

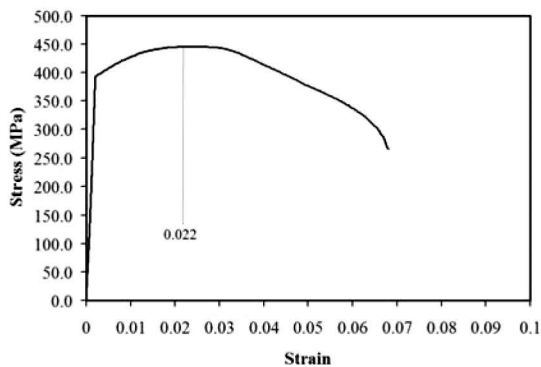


Fig. 9. Stress-strain curve of low carbon steel sheet after two passes of pressing in corrugation dies.

4. Conclusion

The main findings of this research can be presented as follows:

- The grain size of steel sheets is decreased by increasing the pass number. The rate of grain refinement in the first stages is rapid and by increasing the pass number is decreased.

- Yield stress and UTS of sheets are increased during straining until second pass and further deformation than that causes the strength to drop, while the hardness is increased continuously with an increase in the pass number.

- The pressing in corrugation dies process causes the work hardening rate to decrease and the strain rate sensitivity to increase compared to that of as-received specimen.

- By imposing a strain magnitude of 4.64, a deformed sheet with grain size of 230 nm and ultimate tensile strength of 400 MPa is obtained.

Acknowledgements

The authors wish to thank the research board of Sharif University of Technology for the financial support and the provision of the research facilities used in this work.

References

- [1] R. Z. Valiev, R. K. Islamgaliev, and I. V. Alexandrov: *Prog. Mater. Sci.*, 45 (2000), 103.
- [2] E. Rafizadeh, A. Mani, and M. Kazeminezhad: *Mater. Sci. Eng., A*, 515 (2009), 162.
- [3] P. G. Sanders, G. E. Fougere, L. J. Thompson, J. A. Eastman, and J. R. Weertman: *Nanostruct. Mater.*, 8 (1997), 243.
- [4] R. Z. Valiev and T. G. Langdon: *Prog. Mater. Sci.*, 51 (2006), 881.
- [5] Z. Zhang, F. Zhou, and E. J. Lavernia: *Metall. Mater. Trans. A*, 34A (2003), 1349.
- [6] P. Mukherjee, A. Sarkar, P. Barat, S. K. Bandyopadhyay, P. Sen, S. K. Chattopadhyay, P. Chatterjee, S. K. Chatterjee, and M. K. Mitra: *Acta Mater.*, 52 (2004), 5687.
- [7] E. Hosseini and M. Kazeminezhad: *Mater. Sci. Eng. A*, 526 (2009), 219.
- [8] V. Rajinikanth, G. Arora, N. Narasaiah, and K. Venkateswarlu: *Mater. Lett.*, 62 (2008), 301.
- [9] Y. Saito, N. Tsuji, H. Utsunomiya, T. Sakai, and R. G. Hong: *Scr. Mater.*, 39 (1998), 1221.
- [10] D. H. Shin, J.-J. Park, Y.-S. Kim, and K.-T. Park: *Mater. Sci. Eng., A*, 328 (2002), 98.
- [11] P. Mukherjee, A. Sarkar, and P. Barat: *Mater. Charact.*, 55 (2005), 412.
- [12] Y. Fukuda, K. Oh-ishi, Z. Horita, and T. G. Langdon: *Acta Mater.*, 50 (2002), 1359.
- [13] G. Dieter: *Mechanical Metallurgy*, McGraw-Hill book Company, New York, (1986), 351.